

Supporting Information

The Structure Effect of Antifouling Functionalities on the Electrochemical and Antifouling Performances of Conducting Polymers

Ya-Qiong Zhang,[‡] Hsing-An Lin,^{‡,} Qi-Chao Pan, Si-Hao Qian, Shouyan Zhang, Ao Zhuang, Shu-Hua Zhang, Gao Qiu, Maciej Cieplak, Piyush S. Sharma, Yaopeng Zhang, Haichao Zhao,* Bo Zhu**

Y.-Q. Zhang, A. Zhuang, Prof. G. Qiu, Prof. Z. You, Prof. Y. Zhang,
State Key Laboratory for Modification of Chemical Fibres and Polymer Materials & College of
Materials Science and Engineering, Donghua University
2999 Renmin North Road Songjiang, Shanghai 201600

Y.-Q. Zhang, Q.-C. Pan, S.-H. Qian, S.-Y. Zhang, S.-H. Zhang, Prof. H.-A. Lin, Prof. B. Zhu
School of Materials Science and Engineering, Shanghai University
99 Shangda Road, Baoshan, Shanghai 200444
E-mail: halin@shu.edu.cn; bozhu@shu.edu.cn

Dr. M. Cieplak, Dr. Piyush S. Sharma,
Institute of Physical Chemistry, Polish Academy of Sciences (IPC PAS), Kasprzaka 44/52, 01-224
Warsaw, Poland

Dr. H. Zhao
Key Laboratory of Marine Materials and Related Technologies, Zhejiang Key Laboratory of
Marine Materials and Protective Technologies, Ningbo Institute of Materials Technology and
Engineering, Chinese Academy of Sciences, Ningbo 315201, China
E-mail: zhaohaichao@nimte.ac.cn

[‡] These authors contributed equally to this work.

KEYWORDS: antifouling, poly(3,4-ethylenedioxythiophene), zwitterion, oligo(ethylene glycol), phosphorylcholine.

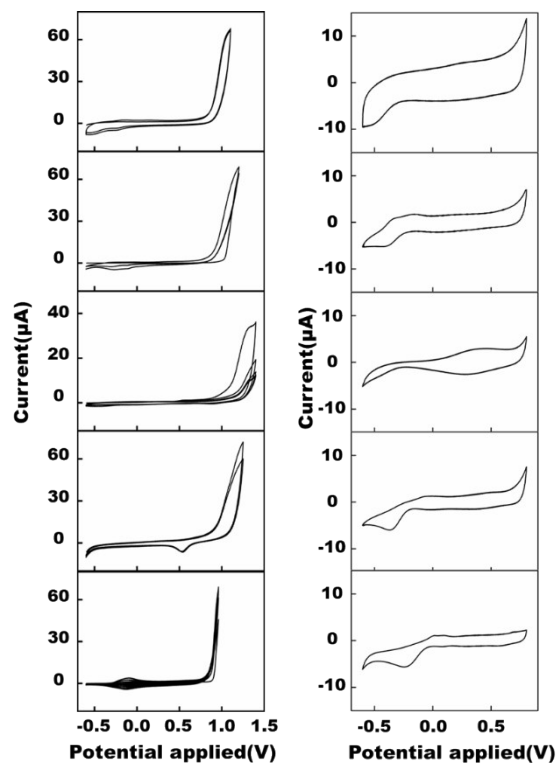


Figure S1. Cyclic voltammograms registered during the electropolymerization of (a) EDOT and antifouling EDOT polymers including (b) EDOT-EG3, (c) EDOT-EG4, (d) EDOT-SB, (e) EDOT-PC; CV profiles of PEDOT polymers in PBS buffer (pH=7.2): (a') PEDOT, (b') PEDOT-EG3, (c') PEDOT-EG4, (d') PEDOT-SB, (e') PEDOT-PC.

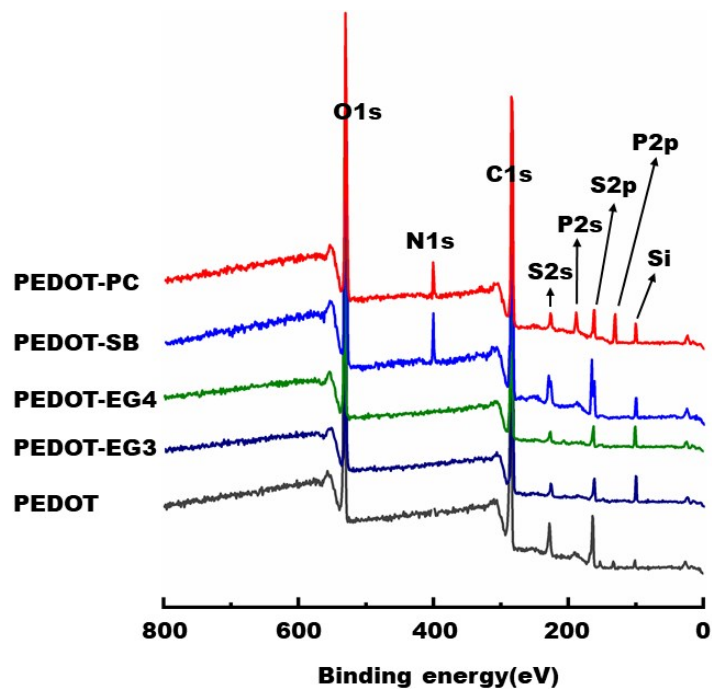


Figure S2. XPS profiles of PEDOT, PEDOT-EG3, PEDOT-EG4, PEDOT-SB, and PEDOT-PC thin films.

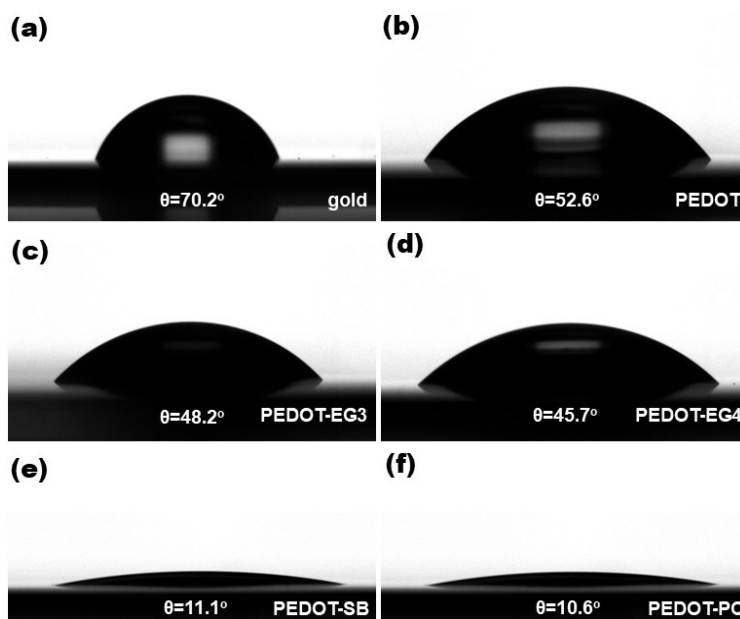


Figure S3. Water contact angles of (a) gold, (b) PEDOT, (c) PEDOT-EG3, (d) PEDOT-EG4, (e) PEDOT-SB, and (f) PEDOT-PC thin films on the microelectrode arrays.

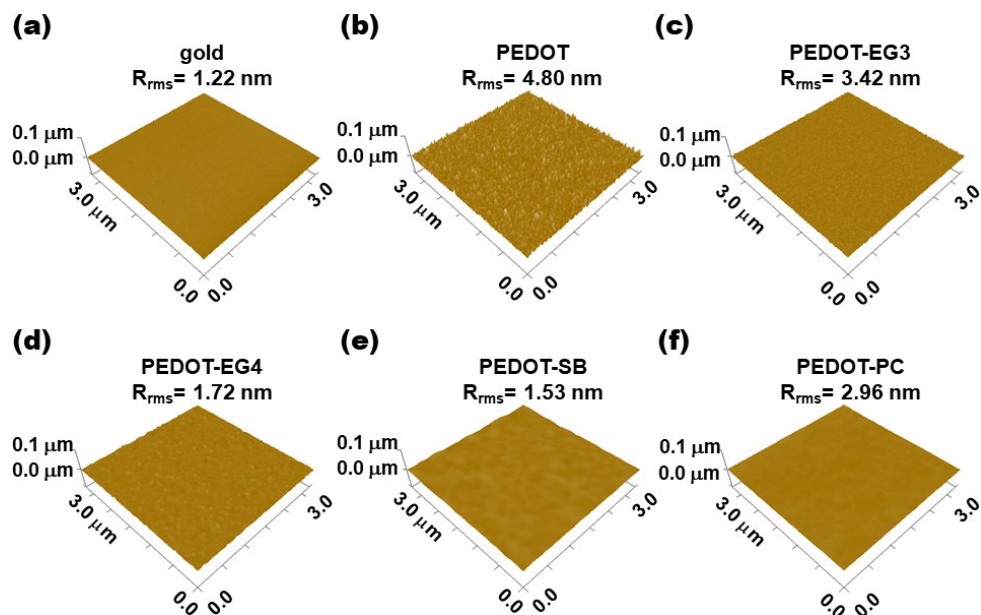


Figure S4. AFM images of PEDOT, PEDOT-EG3, PEDOT-EG4, PEDOT-SB, and PEDOT-PC thin films on the microelectrode arrays.

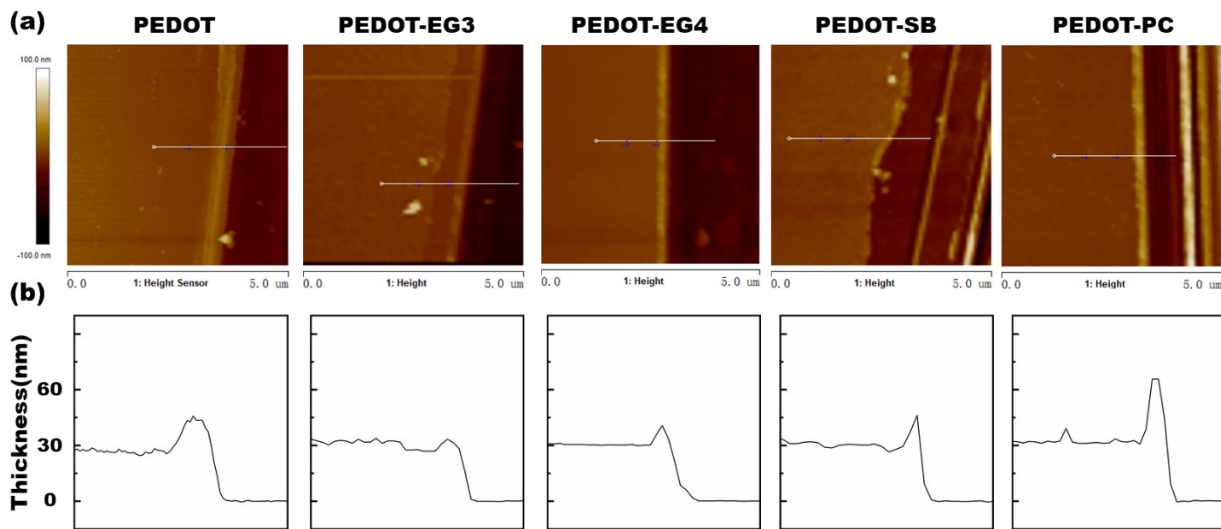


Figure S5. (a) Nanometrological AFM images of PEDOTs thin films (scan range: $5\ \mu\text{m} \times 5\ \mu\text{m}$). (b) Line profiles of step height calculation for PEDOTs thin films.

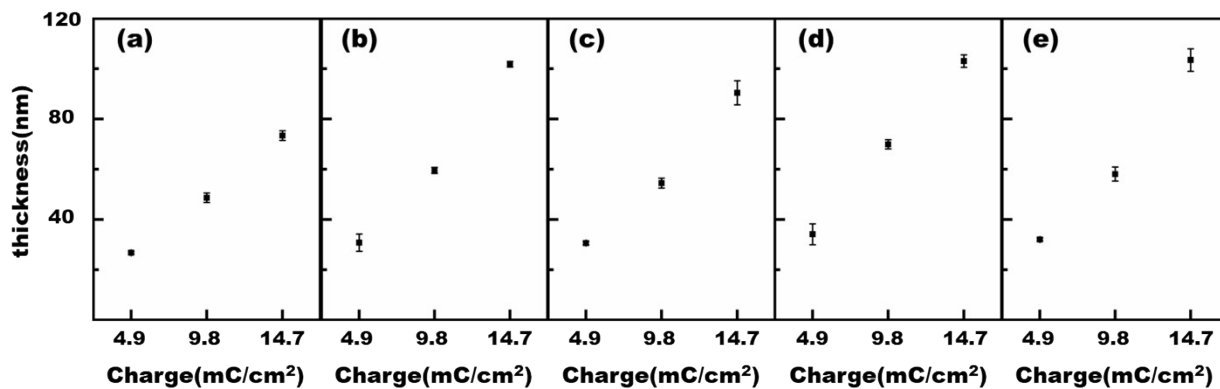


Figure S6. The thickness of (a) PEDOT, (b) PEDOT-EG3, (c) PEDOT-EG4, (d) PEDOT-SB, (e) PEDOT-PC films on the microelectrode arrays at different deposited charge, 4.9, 9.8, and 14.7 mC/cm².

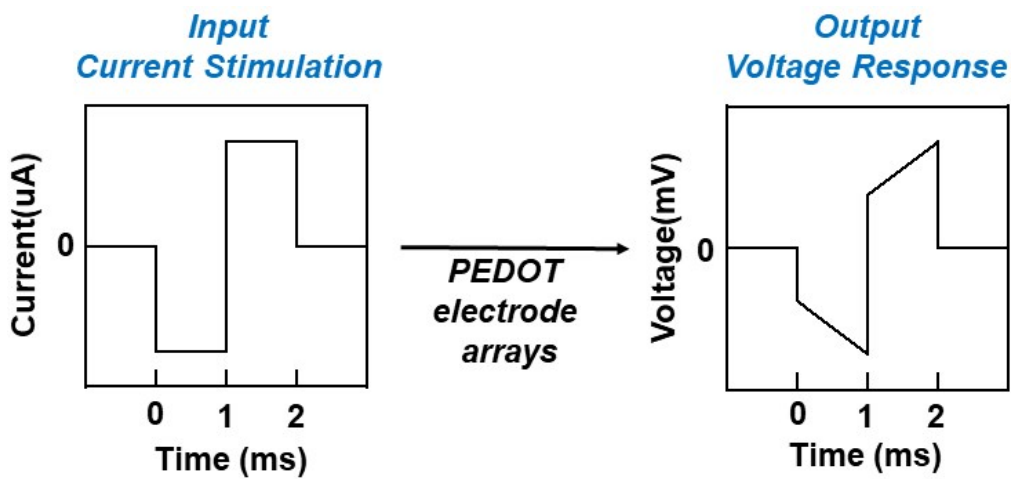


Figure S7. Waveform of biphasic current pulse stimulation.

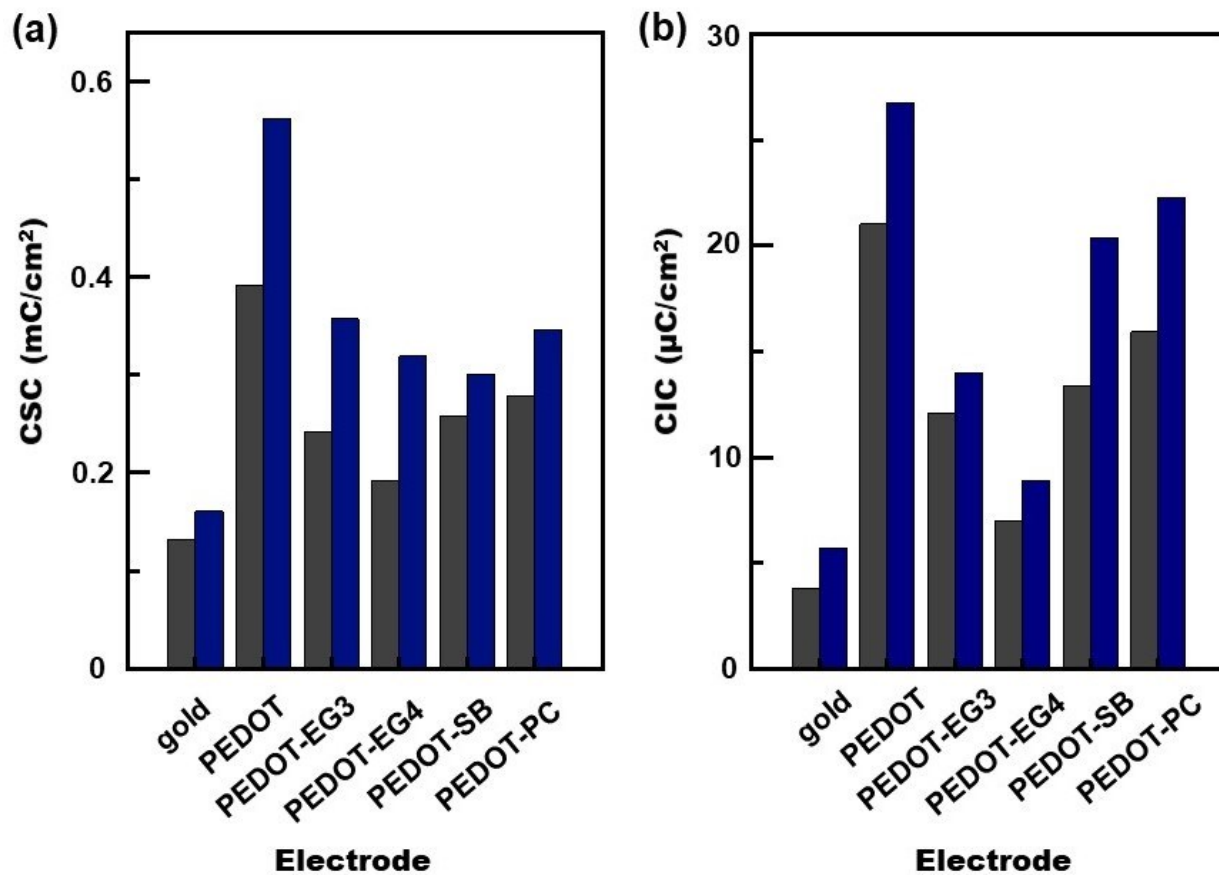


Figure S8. Assessment of (a) charge storage capacities (CSC) and (b) charge injection capacities (CIC) for different electrodes before (gray color) and after electrical stimulation (blue color).

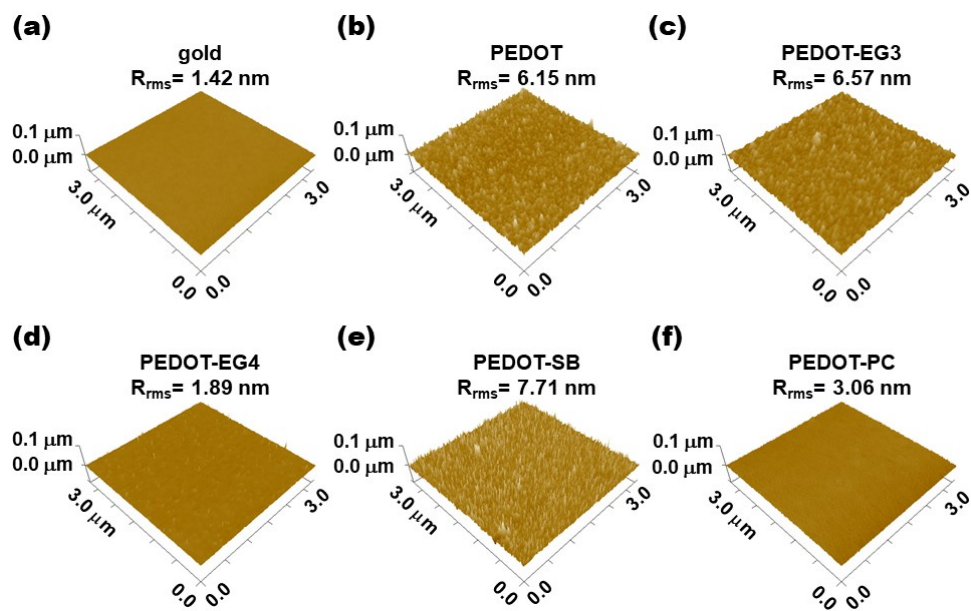


Figure S9. AFM images of PEDOT, PEDOT-EG3, PEDOT-EG4, PEDOT-SB and PEDOT-PC thin films on the microelectrode arrays after the biphasic stimulation.

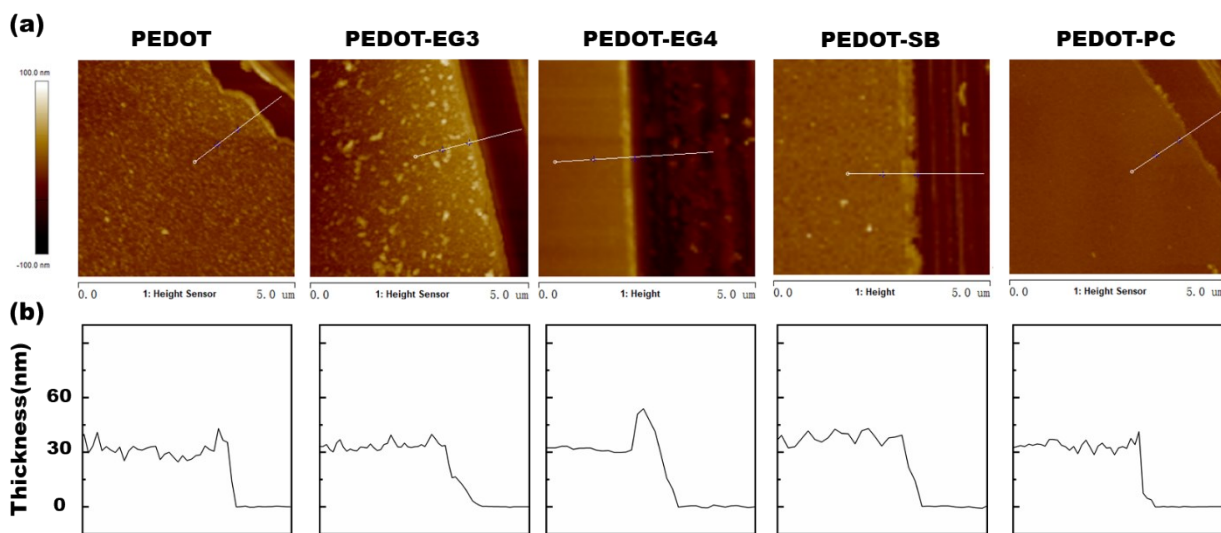


Figure S10. (a) Nanometrological AFM images of PEDOTs thin films after the biphasic stimulation (scan range: $5 \mu\text{m} \times 5 \mu\text{m}$). (b) Line profiles of step height calculation for PEDOTs thin films after the biphasic stimulation.

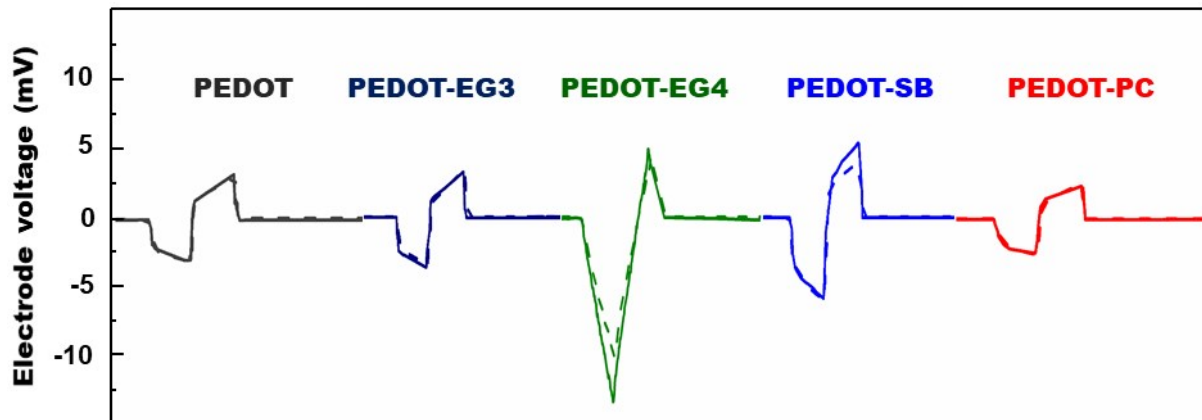


Figure S11. The voltage response of PEDOT, PEDOT-EG3, PEDOT-EG4, PEDOT-SB, and PEDOT-PC electrodes before (solid line) and after (dash line) the biphasic stimulation.

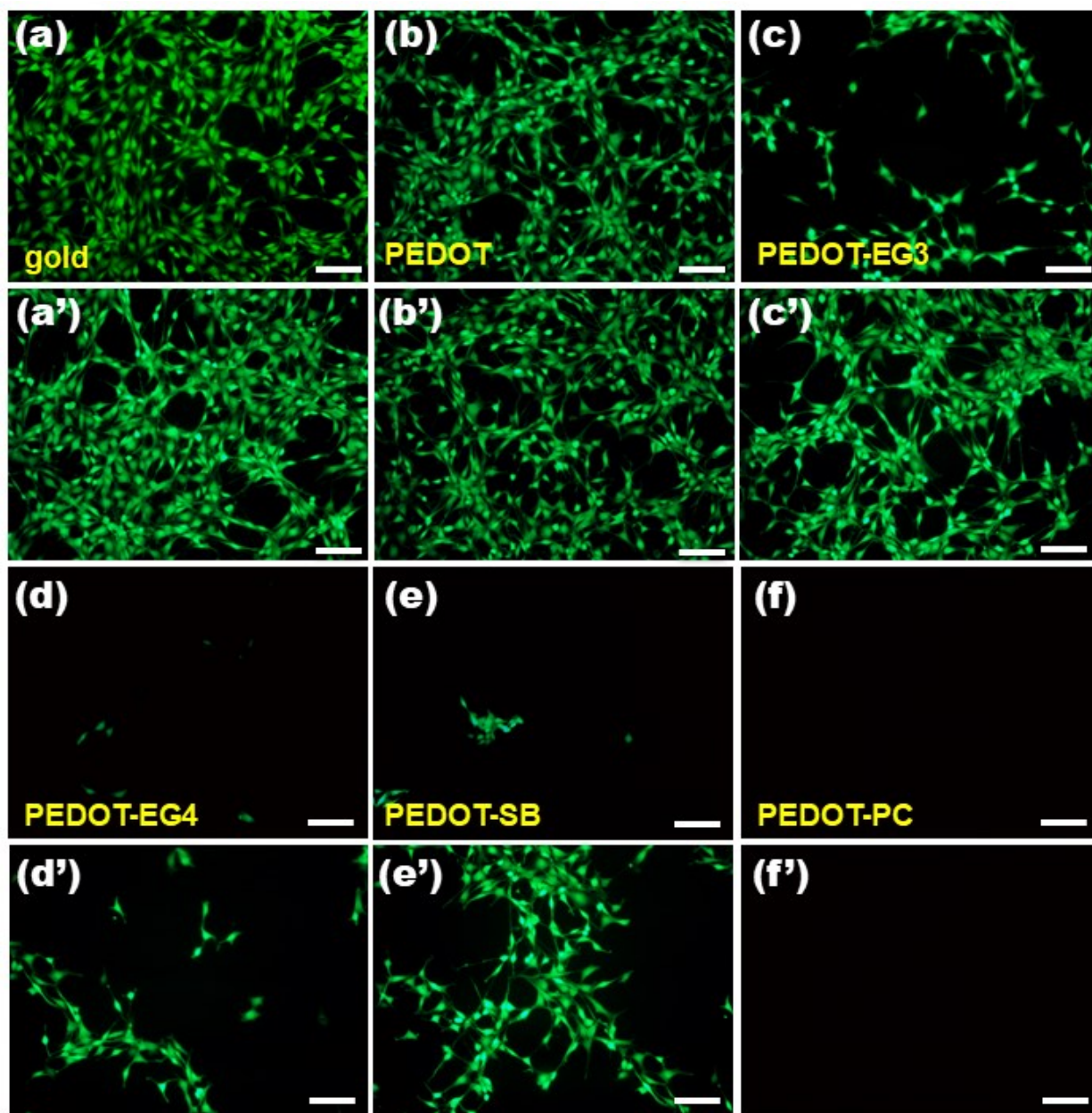


Figure S12. Fluorescence images of NIH 3T3 cells cultured on the gold, PEDOT and antifouling PEDOT electrodes before (a-f) and after (a'-f') the biphasic stimulation: (a, a') gold electrode, (b, b') PEDOT electrode, (c, c') PEDOT-EG3 electrode, (d, d') PEDOT-EG4 electrode, (e, e') PEDOT-SB electrode and (f, f') PEDOT-PC. Green color represents a live cell; red color represents a dead cell. The scale bar is 100 μm .